Frequency calibration of terahertz time-domain spectrometers

M. Naftaly,[1,*] R. A. Dudley,[1] J. R. Fletcher,[2] F. Bernard,[1] C. Thomson,[1] and Z. Tian[1]

[1]*National Physical Laboratory (NPL), Teddington TW11 0LW, UK*
[2]*Department of Physics, University of Durham, Durham, UK*
[*]*Corresponding author: mira.naftaly@npl.co.uk*

Received November 19, 2008; revised March 5, 2009; accepted May 11, 2009;
posted May 29, 2009 (Doc. ID 104230); published June 15, 2009

We present three techniques of calibrating frequency and spectral profile measurements of terahertz time-domain spectrometers. The first utilizes the etalon effect generated by multiple reflections in thin nonabsorbing samples. The second employs a CO gas cell to provide multiple narrow absorption lines at known frequencies. The third aims to use a grating monochromator to produce an independently measured comparable spectrum. © 2009 Optical Society of America

OCIS codes: 120.3940, 120.6200, 300.6495.

1. INTRODUCTION

The terahertz time-domain spectrometer (THz TDS) has emerged as a key measurement device for spectroscopic investigations in the frequency range of 0.1 to 3 THz [1–3]. Measurements with a TDS are made in the time domain using a pump-probe configuration, typically in conjunction with electro-optic sampling for signal detection. Conversion from the time-domain data to a frequency spectrum is achieved by applying the Fourier transform, calculated numerically using the fast Fourier transform (FFT) algorithm.

Calibrating the frequency scale of a THz TDS is possible in principle by adopting techniques used in high-speed electrical signal calibration [4,5]. However, dispersion of both terahertz and optical pulses within the TDS setup, coupled with the numerical errors entailed in applying FFT, introduce characterization uncertainties that can be difficult to quantify [6]. Furthermore, spectroscopic measurements using TDS commonly address complex spectra and seek to determine spectral profiles as well as peak frequencies. It has been shown that errors in the measurements of relative amplitudes may arise from a variety of sources and may be frequency dependent [7]. Therefore, an independent method of verifying spectral measurements obtained by a TDS is required.

In this paper we investigate three approaches for validating the spectral measurements of a TDS system. The first one is a self-contained TDS testing technique employing the etalon effect. The second one uses a known gas spectrum as a calibration standard. The third one utilizes a transfer measurement device, or artifact, characterized by an independent terahertz spectrometer.

2. TERAHERTZ TDS

The National Physical Laboratory (NPL) TDS follows the design of many other groups [8], incorporating a femtosecond laser, a 300 mm optical delay line, a biased GaAs emitter, electro-optic detection using a ⟨110⟩ ZnTe crystal, and a configuration of four 90° parabolic mirrors to guide THz radiation. In the described experiments, data acquisition was achieved by sweeping, rather than stepping, the delay line, thus allowing for faster scan times.

The maximum frequency resolution of a TDS system is given by $c/2L_{\max}$, where $L_{\max}$ is the maximum available length of the delay sweep. In principle, given an arbitrarily long delay line, the resolution of a TDS is ultimately limited by the repetition rate of the pump laser, which is typically around 80 MHz for femtosecond lasers. However, in practice, the achievable resolution is much lower and is set by the noise floor of the system [9]. In common experimental practice, $L_{\max}$ is the delay where the THz signal remains at least a factor of 2 above the noise floor of the detector. In the case of the NPL TDS system this extends beyond 100 mm, allowing a frequency resolution of 1.5 GHz to be achieved.

The frequency scale of the TDS is obtained from the position of the optical delay line. Therefore the minimum frequency uncertainty is determined by the uncertainty in the displacement of the delay line. However, in practice there may be additional sources of frequency error. The conversion of the time-domain trace into spectral and phase information involves applying FFT to the data. The FFT numerical algorithm carries inherent errors associated with the selection of data interval and scan length, and is liable to amplify small errors in the time-domain data. Such errors in the measurement of the THz field amplitude may arise from dispersion in the optical components, from spatial and temporal deviation of the THz and optical beams from the ideal Gaussian pulse-shape, and from nonlinearities in the detector, with all these leading to a distortion of the acquired time-domain profile. The FFT algorithm will then convert these time-domain uncertainties into frequency errors that are difficult to quantify [6]. Although a formalism capable of

quantifying such errors has been developed [5], in practice the calculations are difficult, and it remains far easier, quicker, and more reliable in the context of a TDS to use a calibration standard.

3. TDS FREQUENCY TEST USING ETALON

A potentially self-contained test capable of verifying the frequency scale and the spectral amplitude profile of TDS systems can be performed using a simple etalon-based technique. The test utilizes the occurrence of secondary peaks produced by multiple reflections in thin plane-parallel samples inserted in the THz beam.

It is a well-known phenomenon in TDS systems that multiple reflections in plane-parallel thin samples give rise to etalonlike oscillations in the calculated spectrum. The problem of removing these oscillations from the measured spectra has been extensively addressed, and a number of solutions have been suggested [10–12]. Here etalon oscillations are utilized for the verification of the TDS frequency and amplitude scales.

The method is based on the fact that etalon peaks and troughs in the calculated spectrum occur at frequencies of [12]

$$f_N = \frac{c}{2nl}N, \quad (peaks),$$

$$f_{N+1/2} = \frac{c}{2nl}\left(N + \frac{1}{2}\right), \quad (troughs), \tag{1}$$

where n is the refractive index of the etalon material and l is its thickness. The integer N is the order of the peak, corresponding to the number of wavelengths in a CW etalon. If the sample thickness and refractive index are known, the order N can be identified, and the peak frequencies can be calculated.

The refractive index can be calculated from the time-domain data. However, in TDS both the frequency spectrum and the refractive index are derived from the position of the delay line, so the two quantities are interrelated and subject to the same uncertainties in the position measurement. As a consequence, the frequencies given by Eq. (1) can be used for calibration only if the refractive index is known from an independent measurement.

Additional information is provided by the transmission profile. The transmission spectrum of an etalon as a function of frequency f is given by [13]

$$T = \left(1 + F\sin^2\frac{\delta}{2}\right)^{-1},$$

$$F = \frac{4R}{(1-R)^2},$$

$$R = \left(\frac{n-1}{n+1}\right)^2,$$

$$\delta = 4\pi nlf/c. \tag{2}$$

The peak/trough frequencies can provide frequency calibration, while the transmission spectrum can verify the measurement of the spectral amplitude profile.

A possible alternative approach is to derive the refractive index from the spectral profile of the etalon transmission function by fitting Eq. (2) to the data based only on the sample thickness. It must be noted, however, that this procedure is warranted only if the linearity of the amplitude measurement has been independently tested and confirmed [7]. Nevertheless, such fitting of frequency to the model of Eq. (2) using only sample thickness can in principle provide a route for a self-contained traceable frequency calibration of a TDS [14].

In this experiment the etalon was a GaAs wafer with a thickness of 0.518 mm. The refractive index was obtained from [15] and was also measured by the NPL TDS. The two values were found to agree below 2 THz (which was the range given in [15]); therefore, above 2 THz the NPL value was employed. The average value of the refractive index was 3.60, giving the finesse of 2.6. The time-domain scan length was 80 mm, giving a TDS frequency resolution of 2 GHz.

The two parameters contributing to the uncertainty in the calculated frequency are the wafer thickness and the refractive index. The uncertainty in the measurement of the wafer thickness is ±1 μm. The uncertainty in the refractive index is more difficult to quantify; however, both the results in [15] and the NPL data indicate that it is <0.002. The combined uncertainty in the calculated peak interval is therefore 0.2 GHz. The resulting error in the peak position is cumulative, equal to the interval error times peak order, and will appear as a systematic linearly increasing shift in the observed peak position relative to the calculated value. In contrast, the largest uncertainty in the peak/trough frequencies measured by TDS is the resolution of the system, which in this experiment was 2 GHz and should appear as random noise.

Figure 1 presents part of the observed transmission spectrum of the GaAs wafer together with the calculated

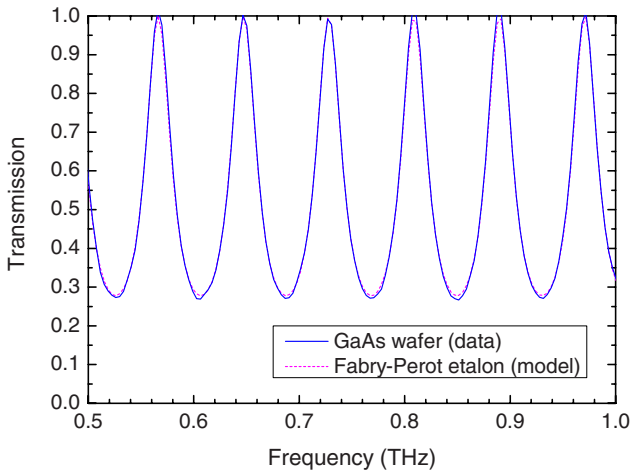

Fig. 1. (Color online) The measured transmission spectrum of a GaAs wafer and the Fabry–Perot etalon model.

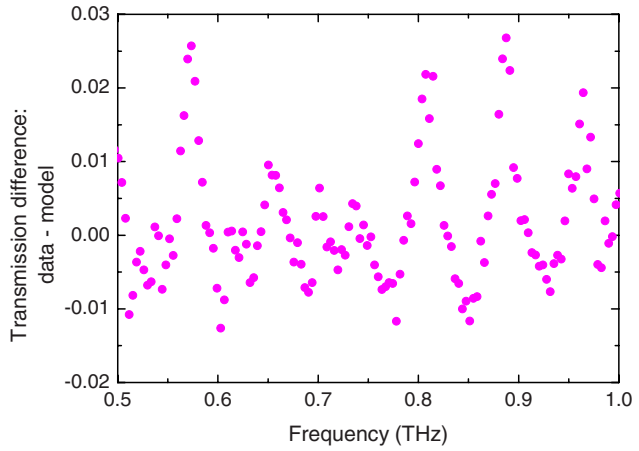

Fig. 2. (Color online) Difference between the measured and calculated transmission values, as shown in Fig. 1.

etalon transmission Eq. (2). Figure 2 plots the difference in transmission between the data and the model, showing that the data agrees with the model to within 2%. The excellent agreement between the measured spectrum and model thus confirms that both the frequency scale and the spectral profile produced by the TDS are correct.

Figure 3 presents the frequency error in the peaks/troughs of the measured spectrum, calculated as the difference between the frequency given by Eq. (1) and the measured peak/trough position. It is seen that, at frequencies below 1.5 THz, the error is 2 GHz or less, i.e., within the resolution of the TDS system. The errors become larger when the system approaches its noise floor at higher frequencies above 1.5 THz. These results therefore confirm that the frequency scale of the TDS is correct within the resolution of the system over its bandwidth up to 1.5 THz. The experiment demonstrates the suitability of the etalon test for verifying the frequency accuracy and spectral profile measurement of a TDS system. The etalon-based method has the advantages of ease and convenience of implementation, and it requires no specialized calibration standards. However, a significant disadvantage is its relatively low frequency resolution, which is limited by the low finesse of the etalon. A low finesse is necessitated by the requirement that the secondary peak be sufficiently large to be measured accurately.

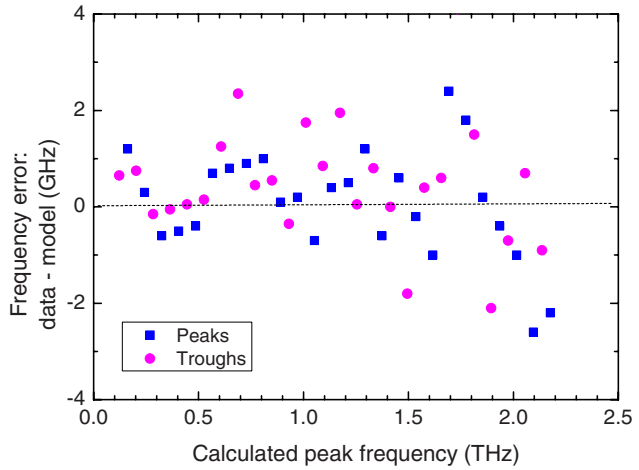

Fig. 3. (Color online) Frequency differences between the measured etalon peaks/troughs and the calculated values.

4. CARBON MONOXIDE ABSORPTION

As noted above, the frequency resolution of the etalon is limited by its finesse. A high-resolution frequency standard should possess a number of narrow absorption lines across the terahertz band. Such spectrum may be provided by a gas whose molecular transitions give rise to multiple absorption peaks with sub-GHz linewidths. In general, THz absorption coefficients in gases are low, therefore requiring large interaction lengths for measurement and making realization impractical.

Perhaps the best known and widely used gas for frequency verification in the THz band is atmospheric water vapor, which possesses many strong narrow lines. However, although the frequencies of these lines are well known [16,17], their relative amplitudes vary with environmental conditions [18] such as atmospheric pressure and humidity. Moreover, many of the lines are doublets and triplets, and therefore require very high (sub-GHz) frequency resolution to define their peak maxima and profiles. The spacing of lines is particularly dense at higher frequencies above 2 THz, where the reduced signal-to-noise ratio and dynamic range of a TDS make accurate measurements far more difficult. Furthermore, the focus of this study was to investigate stable, controllable, well-defined calibration standards. Ambient humidity clearly cannot serve in such role. A sealed air cell with defined humidity is a possible solution, but over time, and if subject to temperature fluctuations, water adsorption on the cell surfaces may alter its moisture content. It was decided therefore to search for another suitable gas.

An investigation of the HITRAN [19] database led us to choose carbon monoxide (CO) gas for this study. While it is toxic in high concentrations, its risks are lower than those of other candidate gases such as N_2O, NO, HCl, or HF. The CO absorption spectrum consists of a series of $J'-J''$ transitions producing lines that are equally spaced in frequency and possess a characteristic amplitude envelope. These transitions have been measured in the range of 0.1–5 THz using laser spectroscopy [20], with the resolution of <10 Hz. The line spacing was determined to be 114 GHz. Subsequent modeling using PGOPHER [21] agreed with the measured peak frequencies to within 1 GHz.

In the present experiment, CO transmission spectrum at a pressure of 3 bar was measured using a 300 mm cell with HDPE windows. Figure 4 presents the CO transmission spectrum measured by TDS. The peak positions as quoted in [20] are indicated by dashed lines. The TDS resolution in this experiment was 1.5 GHz. Excellent agreement is seen between the spectra measured by TDS and by high-resolution laser spectroscopy of [9]. In addition, the characteristic amplitude envelope is clearly observed.

Additional confirmation is provided by the result shown in Fig. 5, which plots the observed frequency of each CO line against the upper transition level number J'. The data in Fig. 5 are seen to be linear with the slope of 114 GHz. Also plotted in Fig. 5 are the differences between the peak positions as measured by TDS and those

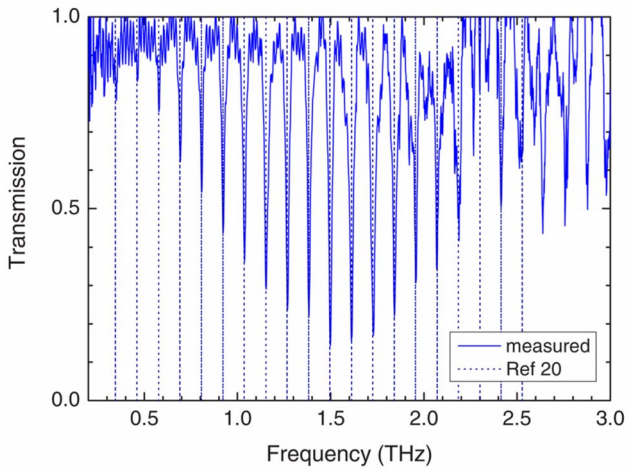

Fig. 4. (Color online) Transmission spectrum of carbon monoxide measured by TDS. Peak positions from [20] are indicated by vertical lines.

quoted in [20]. The mean error of the TDS data is 2 GHz, which is comparable with the system resolution of 1.5 GHz. However, as in the previous case, the errors increase steeply at frequencies above 2 THz where the TDS system approaches its noise floor. These results demonstrate the suitability of a CO gas cell for high-resolution frequency calibration of TDS systems.

5. TERAHERTZ MONOCHROMATOR

In addition to the above methods of TDS calibration, it was deemed desirable to build an independent instrument capable of direct spectral measurements, which would be comparable with TDS results and would provide a straightforward means of traceable frequency verification. The selected technique had to be capable of measuring short-pulse broadband sources, to compare with those employed in TDS, while minimizing harmonic errors. The grating-based monochromator emerged as a simple solution with the ability to convert the broadband signal into an easily configurable wavelength measurement. The important distinction between a TDS and a monochromator is that measurement by TDS proceeds via FFT conversion from time domain into frequency; and moreover, every data point of the resulting frequency spectrum is affected by every point of the time-domain trace. In contrast, the monochromator determines the spectral power at each wavelength directly and independently as a simple function of the grating angle.

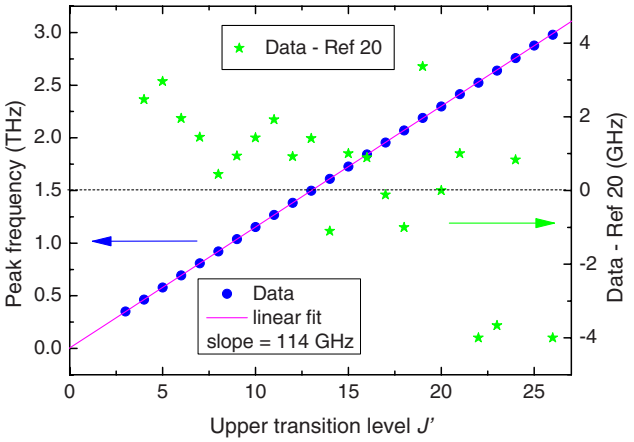

Fig. 5. (Color online) Left ordinate: CO absorption line frequencies as a function of the upper transition level J', showing a constant spacing of 114 GHz. Right ordinate: Frequency differences between the measured peaks and those given in [20].

A monochromator was built using the Czerny–Turner configuration utilizing a reflection grating [22] and two 90° off-axis parabolic mirrors. The grating was a machined stainless steel with a line period of 0.75 mm and a blaze angle of 16.25°. The terahertz source was a biased GaAs emitter similar to that used in the TDS. The signal was monitored by a Golay cell with the detector aperture serving as the exit slit.

Spectral measurements using a grating monochromator are made by rotating the grating while recording the detected signal as a function of the angle. The relationship between the grating angle α and the frequency f of the beam falling on the detector is given by [22]

$$f(\alpha) = \frac{kc}{2p\,\sin(\alpha/2)\cos(\delta/2)}, \tag{3}$$

where p is the grating pitch, k is the diffractive order ($k=1$ in the NPL monochromator), and c is the speed of light. The angle δ is the angle of first-order reflection, termed the deviation angle, which is a constant and a function of the instrument geometry. In the NPL monochromator this angle is $\delta = 11 \pm 1°$. The angle α is the variable in spectral measurements.

The resolution of a monochromator is limited primarily by linear dispersion, i.e., by the presence of a bandwidth of frequencies in the beam entering the detector aperture. The monochromator bandpass is determined by its geometry and, unlike the TDS, is a function of the central frequency f [22]:

$$\frac{\mathrm{d}f}{\mathrm{d}x} = \frac{f^2 p}{cF_B}\cos\frac{1}{2}(\alpha+\delta), \tag{4}$$

where x is measured perpendicular to the beam in the exit focal plane, and F_B is the focal length of the exit parabolic. In our case, $\mathrm{d}x$ is the aperture of the Golay cell (3 mm). Using Eq. (4), the resolution of the monochromator is calculated to be 13 GHz at 0.5 THz and 50 GHz at 1 THz. The resolution can be improved by introducing a vertical slit in front of the detector (thus decreasing $\mathrm{d}x$). However, this reduces the signal and therefore lowers the dynamic range of the instrument. More importantly, the minimum effective slit width is set by the diffraction limit, which at 0.5 THz is 2.4 mm. As this is close to the aperture diameter of the Golay cell, it was decided to dispense with an exit slit.

The monochromator was tested using the CO gas cell. Figure 6 presents a part of the transmission spectrum of CO, measured in the TDS system, together with that obtained by the monochromator. The TDS spectrum shown in Fig. 6 was squared for correct comparison with the monochromator, because TDS measures amplitude whereas the monochromator measures power. The ab-

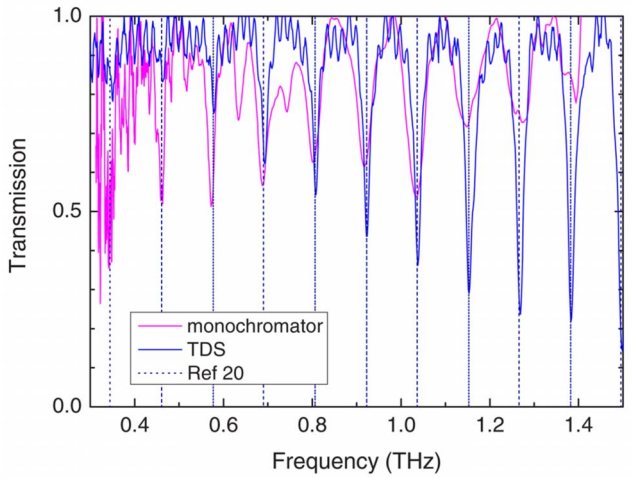

Fig. 6. (Color online) Comparison of CO absorption lines measured by the TDS and the monochromator. Peak positions given by [20] are indicated by vertical lines

sorption lines quoted in [20] are indicated by vertical lines. It is seen that the frequencies obtained by the two instruments agree within the uncertainty of the monochromator. However, the peak profiles and amplitudes differ significantly. The TDS resolution is frequency-independent, and in this experiment was 1.5 GHz. In contrast, the resolution of the monochromator is an order of magnitude lower and further decreases at higher frequencies, thereby causing apparent line broadening and a concomitant reduction in the peak amplitude. Moreover, the bandwidth of the monochromator is only half that of the TDS.

This result demonstrates that a simple grating monochromator cannot serve to verify the frequency scale of a TDS owing to its insufficient frequency resolution and narrow bandwidth. Although improved performance may be achieved by using a more complex design [23], nevertheless a monochromator does not appear to offer a promising frequency calibration route.

6. CONCLUSIONS

We have presented three methods of calibrating the frequency and spectral profile measurement of a TDS. The first method is a potentially self-contained TDS measurement, employing the etalon effect of multiple reflections within a thin plane-parallel sample. The resulting transmission spectrum has multiple evenly spaced peaks and troughs whose frequencies and profiles can be calculated based on the sample thickness and refractive index, providing comparison with the obtained data. The method is easy and convenient to apply, requiring no additional equipment, and was shown to perform well, but it cannot serve for high-resolution frequency calibration.

The second method employs a CO gas cell offering a series of narrow absorption lines with a characteristic spectral profile. The CO gas cell was demonstrated to be a useful standard for high-resolution frequency calibration, but it requires a specially manufactured gas cell.

The third scheme employs a scanning grating monochromator and a transfer artifact, and aims to provide a spectral measurement that is independent of TDS but comparable with it. However, it was seen that, in its present configuration, the resolving power of the monochromator is inadequate to serve as a verification instrument for a TDS.

ACKNOWLEDGMENTS

The authors thank the DTI National Measurement System for financial support under the Electromagnetics Program.

REFERENCES

1. M. C. Beard, G. M. Turner, and C. A. Schmuttenmaer, "Terahertz spectroscopy," J. Phys. Chem. B **106**, 7146–7159 (2002).
2. M. Hangyo, T. Nagashima, and S. Nashima, "Spectroscopy by pulsed terahertz radiation," Meas. Sci. Technol. **13**, 1727–1738 (2002).
3. P. Y. Han and X.-C. Zhang, "Free-space coherent broadband terahertz time-domain spectroscopy," Meas. Sci. Technol. **12**, 1747–1756 (2001).
4. A. J. A. Smith, A. G. Roddie, and D. Henderson, "Electro-optic sampling of low temperature GaAs pulse generators for oscilloscope calibration," Opt. Quantum Electron. **28**, 933–943 (1996).
5. D. F. Williams, A. Lewandowski, T. S. Clement, J. C. M. Wang, P. D. Hale, J. M. Morgan, D. A. Keenan, and A. Dienstfrey, "Covariance-based uncertainty analysis of the NIST electro-optic sampling system," IEEE Trans. Microwave Theory Tech. **54**, 481–491 (2006).
6. H. J. Barker, G. C. Cho, H. Kurz, Q. Wu, and X.-C. Zhang, "Distortion of terahertz pulses in electro-optic sampling," J. Opt. Soc. Am. B **15**, 1795–1801 (1998).
7. M. Naftaly and R. Dudley, "Linearity calibration of amplitude and power measurements in terahertz systems and detectors," Opt. Lett. **34**, 674–676 (2009).
8. G. Zhao, R. N. Schouten, N. van der Valk, W. Th. Wenckebach, and P. C. M. Planken, "Design and performance of a THz emission and detection setup based on a semi-insulating GaAs emitter," Rev. Sci. Instrum. **73**, 1715–1719 (2002).
9. S. Mickan, J. Xu, J. Munch, X.-C. Zhang, and D. Abbott, "The limit of spectral resolution in THz time-domain spectroscopy," Proc. SPIE **5277**, doi:.
10. T. D. Dorney, R. G. Baraniuk, and D. M. Mittleman, "Material parameter estimation with terahertz time-domain spectroscopy," J. Opt. Soc. Am. A **18**, 1562–1571 (2001).
11. W. Withayachumnankul and B. Ferguson, "Direct Fabry-Perot effect removal," Fluct. Noise Lett. **6**, L227–L239 (2006).
12. M. Naftaly and R. E. Miles, "A method for removing etalon oscillations from THz time-domain spectra," Opt. Commun. **280**, 291–295 (2007).
13. R. Guenther, *Modern Optics* (Wiley, 1990).
14. E. N. Grossman and D. G. McDonald, "Partially coherent transmittance of dielectric lamellae," Opt. Eng. (Bellingham) **34**, 1289–1295 (1995).
15. D. Grischkowsy, S. Keiding, M. Van Exter, and Ch. Fattinger, "Far-infrared time-domain spectroscopy with terahertz beams of dielectrics and semiconductors," J. Opt. Soc. Am. B **7**, 2006–2015 (1990).
16. R. J. Foltynowicz and R. E. Allman, "Terahertz time-domain spectroscopy of atmospheric water vapor from 0.4 to 2.7 THz," Sandia Report, SND2005–5709, 2005.
17. D. M. Mittleman, R. H. Jacobsen, R. Neelmani, R. G. Baraniuk, and M. C. Nuss, "Gas sensing using terahertz time-domain spectroscopy," Appl. Phys. B **67**, 379–390 (1998).
18. X. Xin, H. Altan, A. Saint, D. Matten, and R. R. Alfano,

"Terahertz absorption spectrum of *para* and *ortho* water vapors at different humidities at room temperature," J. Appl. Phys. **100**, 094905 (2006).

19. L. S. Rothman, D. Jacquemart, A. Barbe, D. Chris Benner, M. Birk, L. R. Brown, M. R. Carleer, C. Chackerian, Jr., K. Chance, L. H. Coudert, V. Dana, V. M. Devi, J.-M. Flaud, R. R. Gamache, A. Goldman, J.-M. Hartmann, K. W. Jucks, A. G. Maki, J.-Y. Mandin, S. T. Massie, J. Orphal, A. Perrin, C. P. Rinsland, M. A. H. Smith, J. Tennyson, R. N. Tolchenov, R. A. Toth, J. Vander Auwera, P. Varanasi, and G. Wagner, "The HITRAN 2004 molecular spectroscopic database," J. Quant. Spectrosc. Radiat. Transf. **96**, 139–204 (2005).
20. T. D. Varberg and K. M. Evenson, "Laser spectroscopy of carbon monoxide: a frequency reference for the far infrared," IEEE Trans. Instrum. Meas. **42**, 412–414 (1993).
21. PGOPHER, a Program for Simulating Rotational Structure, C. M. Western, University of Bristol, http://pgopher.chm.bris.ac.uk
22. J. M. Lerner and A. Thevenon, "The optics of spectroscopy," Horiba-Jobin-Yvon tutorial: http://www.spexjobinyvon.com/SiteResources/Data/Templates/1divisional.asp?DocID=566&v1ID=&lang=
23. J. W. Russell and H. L. Strauss, "Czerny–Turner far infrared spectrometer for the 300–10 cm^{-1} region," Appl. Opt. **4**, 1131–1136 (1965).